Effects of Misalignment Between Transmission and Emission Scans on Attenuation-Corrected Cardiac SPECT

Ichiro Matsunari, Guido Böning, Sibylle I. Ziegler, Istvan Kosa, Stephan G. Nekolla, Edward P. Ficaro and Markus Schwaiger
Nulearmedizinische Klinik und Poliklinik der Technischen Universität München, Klinikum rechts der Isar, München, Germany; and Department of Internal Medicine, Division of Nuclear Medicine, University of Michigan Medical Center, Ann Arbor, Michigan

Misalignment between transmission and emission scans in attenuation-corrected (AC) cardiac SPECT can introduce errors of measured activity. The severity of these errors, however, has not yet been fully elucidated. **Methods:** We performed a phantom measurement as well as a study of patients with low likelihood of coronary artery disease. Transmission and emission scans were acquired using a triple-head SPECT system with a collimated ^{241}Am line source and an offset fanbeam collimator. The left ventricular myocardium was divided into five segments, and the mean regional activity was calculated for each segment using a semiquantitative polar map approach. Misalignment between transmission and emission data was created by shifting the emission data along the x, y or z axis. **Results:** In the heart phantom, a shift between the transmission and emission data produced a decrease or increase in relative regional activity in each segment resulting in heterogeneous activity distribution. A 7-mm (1-pixel) shift produced up to 15% change in relative regional activity, suggesting that even a small misalignment between transmission and emission data can produce serious errors in measured activity. In the clinical data, the effects of misalignment were less significant than those observed in the phantom data but were still measurable and visually identifiable. **Conclusion:** The results indicate that a small misalignment between the transmission and emission data can produce serious errors in measured activity, and, thus, geometrical precision is essential for accurate diagnosis of AC SPECT images.

Key Words: attenuation correction; SPECT; transmission; emission scans; misalignment

J Nucl Med 1998; 39:411–416

Attenuation artifacts are known to reduce the diagnostic accuracy of cardiac SPECT imaging. Recently, approaches for attenuation correction have been proposed (*1–3*), and clinical results have shown its use for improving the detection of coronary artery disease (*4*) as well as the identification of viable myocardium (*5*). Misalignment between transmission and emission scans, on the other hand, can introduce errors of measured activity into attenuation-corrected (AC) SPECT images. This is particularly true when a sequential acquisition of transmission and emission scans is performed because such misalignment can easily be introduced by patient motion between the transmission and emission scans.

Similar errors between transmission and emission data could also occur in multidetector SPECT systems with simultaneous transmission and emission scan capability if transmission and emission images are acquired using separate heads or if one or more detectors become misaligned. Considering the increasing availability of attenuation correction techniques for cardiac SPECT imaging, it would be useful to know how such misalignment affects AC SPECT images.

Thus, this study was designed to evaluate the effect of errors caused by misalignments between the transmission and emission data on AC cardiac SPECT images acquired over 360°. Because evaluation of SPECT images usually relies on relative regional activity rather than absolute value, we only studied the misalignment effects on relative regional activity.

MATERIALS AND METHODS

Cardiac Phantom

The phantom study was performed using an elliptical cylinder chest phantom (32×23×17.7 cm) (RTW, Freiburg, Germany) with cardiac inserts (Model 7070, Data Spectrum Corp., Chapel Hill, NC). A balloon filled with approximately 200 ml of radioinactive water was also inserted in the right lower part of the chest phantom to simulate diaphragmatic attenuation. The myocardium was filled with 50 MBq (0.45 MBq/ml) ^{99m}Tc. The chest wall, as well as the ventricular cavity, were filled with radioinactive water. The phantom had a chest cavity with air around the heart insert to simulate lungs.

Patients with Low Likelihood of Coronary Artery Disease

Ten patients (8 men, 2 women; age range 50–67 yr; mean age 58 ± 5 yr) with low likelihood (≤5%) of coronary artery disease based on age, sex, history and exercise electrocardiogram were studied (*6*).

Symptom-limited treadmill exercise was performed, and 740-1110 MBq (20–30 mCi) ^{99m}Tc-sestamibi was injected at peak exercise. Imaging was started 20–30 min postinjection using identical acquisition parameters (e.g., scan time, energy window) used for the phantom study.

Data Acquisition

Simultaneous transmission and emission measurement was performed using a triple-head SPECT system (MULTISPECT 3, Siemens AG, Erlangen, Germany) equipped with a low-energy, fanbeam collimator with a focal length of 53 cm with its focal line offset by 17 cm for detector 1 and with low-energy, high-resolution, parallel-hole collimators for detectors 2 and 3 (*5,7,8*). The transmission line source consisted of a 5.55 GBq (150 mCi) ^{241}Am line source sealed in a stainless steel tube.

Transmission and emission projection data were acquired simultaneously in 64×64 matrices. Images were acquired in 6° steps over 360° for 20 sec per projection. An energy window of 59.0 ± 5.9 keV was used for the ^{241}Am transmission photons, and a 15% window centered on the 140-keV peak was used for the emission data. An 80-sec transmission blank scan was acquired to compute attenuation maps from the transmission data.

Received Dec. 12, 1996; revision accepted Jun. 12, 1997.
For correspondence or reprints contact: Markus Schwaiger, MD, Nuklearmedizinische Klinik und Poliklinik der Technischen Universität München, Klinikum rechts der Isar, Ismaninger Str. 22, 81675 München, Germany.

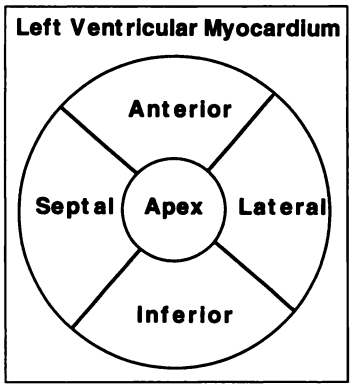

FIGURE 1. Schematic representation of polar map display. The left ventricular myocardium was divided into five segments. After normalizing pixel values for the region showing the maximal activity in the myocardium, the mean relative regional activity was calculated for each segment.

Processing of SPECT Data

Image reconstruction of SPECT data was performed in a manner similar to that previously reported (*4,9*) except for the use of filtered backprojection (FBP) to reconstruct transmission data. Rather than iterative methods, FBP was used to reconstruct the transmission data in this study because the geometry used provided a transmission imaging field-of-view of 39 cm, yielding little truncation of the transmission data, and because FBP requires less computational power compared to iterative reconstruction methods. As previously described by Ficaro et al. (*4*), the main reason for the use of iterative reconstruction for transmission data is to minimize truncation problems, and, theoretically, the use of FBP to reconstruct transmission data should not alter results. After the correction of down scatter from the emission to transmission data, misalignment between transmission and emission data was created by manipulating emission projection data along the x- (right/left), y- (up/down) and z-axis (cephalad/caudal) according to the shift desired. This manipulation produced the effect that would have been obtained had the subject actually moved to the new position between transmission and emission scans. It also represents the situation in which camera heads used for emission acquisition are not aligned to the detector that acquires transmission data. No manipulation was performed for transmission data. The magnitude of the shift ranged from 1 to 5 pixels, where 1-pixel was 7-mm. The emission images were then reconstructed using an iterative reconstruction method [penalized weighted least-squares algorithm (*10*)] with reconstructed attenuation maps to correct the emission data for photon attenuation.

In the setup used in this study, transmission and emission data were acquired simultaneously in different heads. Careful alignment procedure and calibration tools provided by the manufacturer were used to assure data acquisition without misalignment. The calibration tools used in this study included those for source-to-detector distance, fanbeam offset and pixel sizes.

Data Analysis

Image data analysis was performed using a semiquantitative polar map approach, which was developed in our laboratory. This method involved two steps. First, the long axis of the left ventricle was defined interactively in three dimensions. Second, an automatic volumetric radial search for activity maxima was performed (*11*) creating 15 short-axis slices. This procedure was performed by a single operator, and great care was taken to keep a consistent axis in the aligned and misaligned image datasets for each patient. The left ventricular myocardium was then divided into five segments as displayed in Figure 1. The SPECT images were normalized to the pixel showing maximal value in the left ventricular myocardium. The mean relative regional activity was then calculated for each segment. The mean relative regional activity data in each segment without any misalignment served as the control data, while the mean regional activity for each segment from images reconstructed with various misalignments are referred to as the misaligned data. The changes of the mean relative regional activity in each segment between the control and misaligned data were calculated as indices of errors.

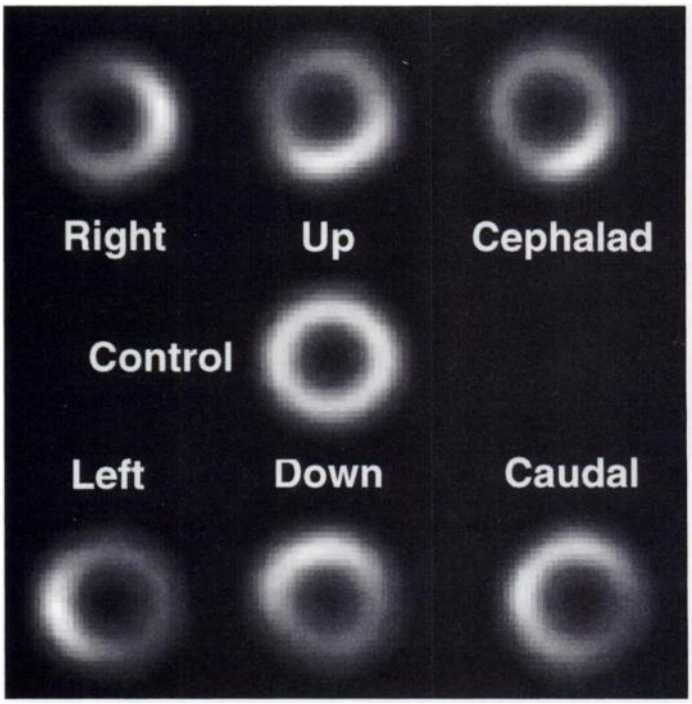

FIGURE 2. Effects of a 21-mm (3-pixel) displacement of the emission data in various directions on a homogeneous cardiac phantom. The control image with no misalignment shows uniform myocardial distribution (center), while misalignment in any direction causes apparent inhomogeneity in myocardial distribution on the reconstructed emission image.

Statistical Analysis

Data were expressed as mean ± s.d. The mean values were compared using a Wilcoxon signed rank test. Statistical significance was defined as $p < 0.05$.

RESULTS

Phantom Study

Reconstructed short-axis slices of the cardiac phantom, with a 21-mm (3-pixel) misalignment in various directions, are displayed in Figure 2. The visual effect of misalignment is readily apparent from the emission images. Changes in relative regional activity from shifting the emission data by various degrees and directions are shown in Figure 3. A shift between the transmission and emission data, regardless of its direction, produced a decrease or increase in relative regional activity in all five segments. Notably, a right shift as small as 7-mm (1-pixel) produced 15% change of relative regional activity in the septal wall. For a given misalignment, the severity of such changes differed from segment to segment resulting in inhomogeneity of activity distribution in the myocardium.

Clinical Study

The effects of misalignment in the human heart from a 21-mm (3-pixel) shift, as was done in the phantom data, are displayed in Figure 4. Similar to the phantom results, inhomogeneity produced by the misalignment between transmission and emission data are visually noted. The degree of change, however, was less significant than that seen in the phantom data. The relationship between the degree of displacement and the severity of errors in relative regional activity on the AC SPECT images is shown in Figure 5. The values are reported as an average from all 10 patients. As was observed in the

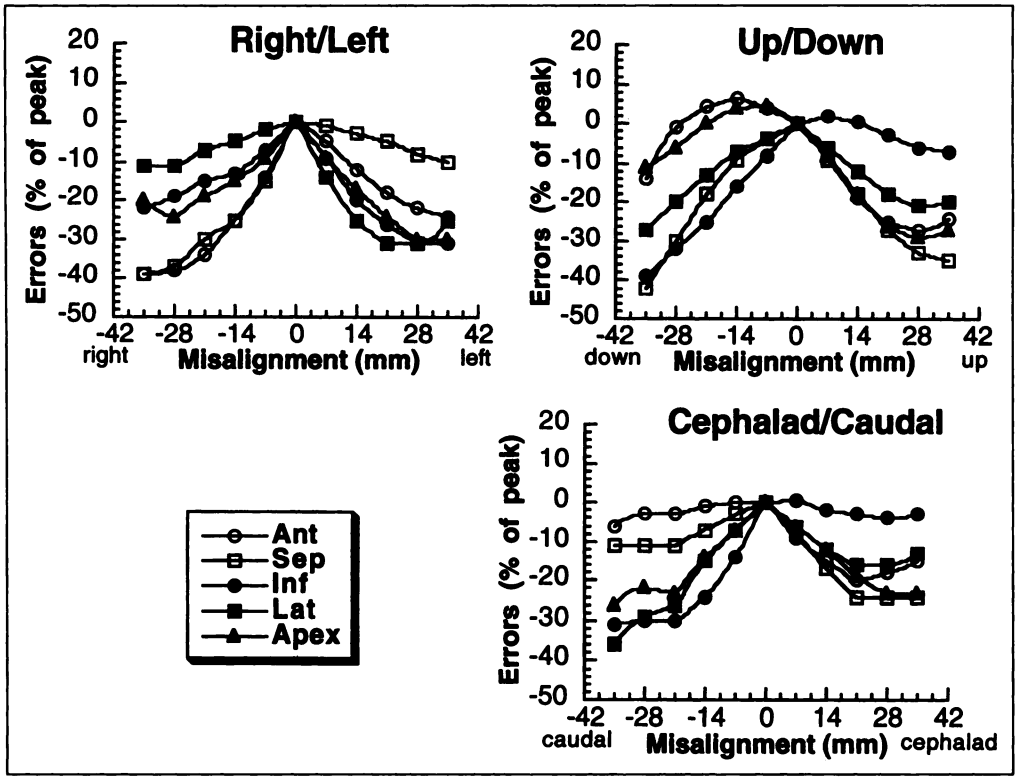

FIGURE 3. Changes in relative regional activity as a function of misalignment between transmission and emission data on a cardiac phantom are shown for each of five segments. The directions shown on each graph indicate the direction in which the emission data have been shifted relative to the transmission data.

phantom data, a shift of the emission data produced changes in relative regional activity. Nevertheless, the effect of misalignment was less significant in patients than in the phantom. For example, a 21-mm (3-pixel) shift produced errors of more than 10% in 1.0 ± 0.6 of the five segments for each direction compared to 3.8 ± 0.4 of the segments in the phantom data ($p = 0.026$). The effect of misalignment along the z-axis (cephalad/caudal), especially in the caudal direction, was less significant than that along the x- (right/left) or y-axis (up/down). However, the effect of shifting the emission data was measurable and visually identifiable in Figures 4 and 5. A 7-mm (1-pixel) right shift, for example, produced a mean 7% ± 5% change in relative regional activity in the septal wall. This increased to a mean of 14% ± 6% when the emission data were shifted by 14 mm (2 pixels).

Tables 1–3 show the effects of misalignment in 10 patients. It is noted that, for a given misalignment, there was a considerable variation in measured errors from patient to patient indicating that the severity of errors is difficult to predict from the magnitude of misalignments in some patients.

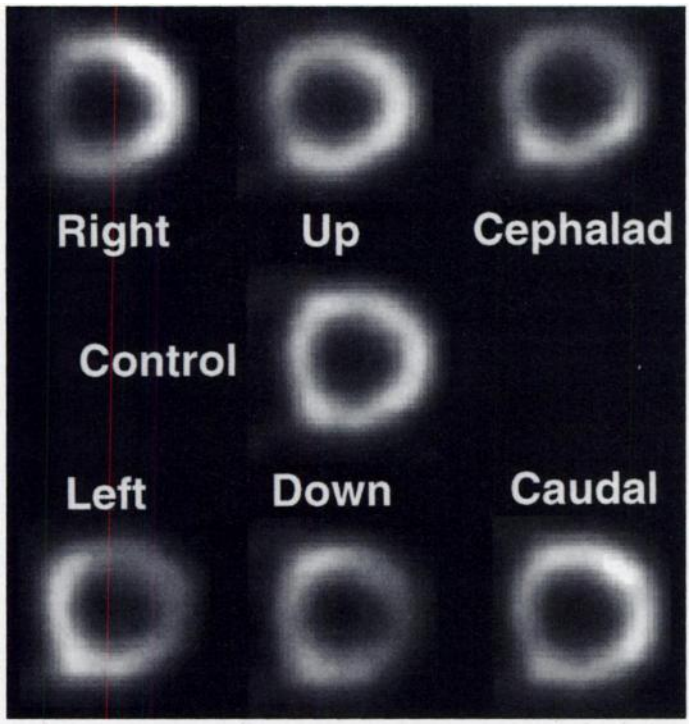

FIGURE 4. Effects of a 21-mm (3-pixel) misalignment on ^{99m}Tc-sestamibi activity distribution from a patient with low likelihood of coronary artery disease. A shift of the emission data relative to the transmission data introduces inhomogeneity in myocardial distribution into the reconstructed emission image.

DISCUSSION

The major findings of this study were: (1) a shift between transmission and emission data, regardless of its direction, produced a decrease or increase in relative regional activity in all five segments; (2) in the cardiac phantom, a 7-mm (1-pixel) shift produced up to 15% change in relative regional activity and (3) the errors in the human heart were less significant than those observed in the phantom but were still measurable.

Effects of Misalignment in the Phantom

Our data clearly show that misalignment between transmission and emission data can cause serious errors in relative regional activity on AC SPECT images. This is consistent with published data by Murase et al. (*12*) who studied the effects of misalignment in a thorax phantom as well as in clinical brain data. A misalignment as small as a 7-mm (1-pixel) shift created up to 15% change in measured activity suggesting that even a small shift can lead to serious errors in measured activity in the AC SPECT images. For a given misalignment, these effects are different in different segments. Some segments decrease in relative regional activity, and others increase resulting in rather markedly inhomogeneous distribution in the myocardium. Thus, geometrical precision between transmission and emission data is critical for the accurate measurement of AC SPECT

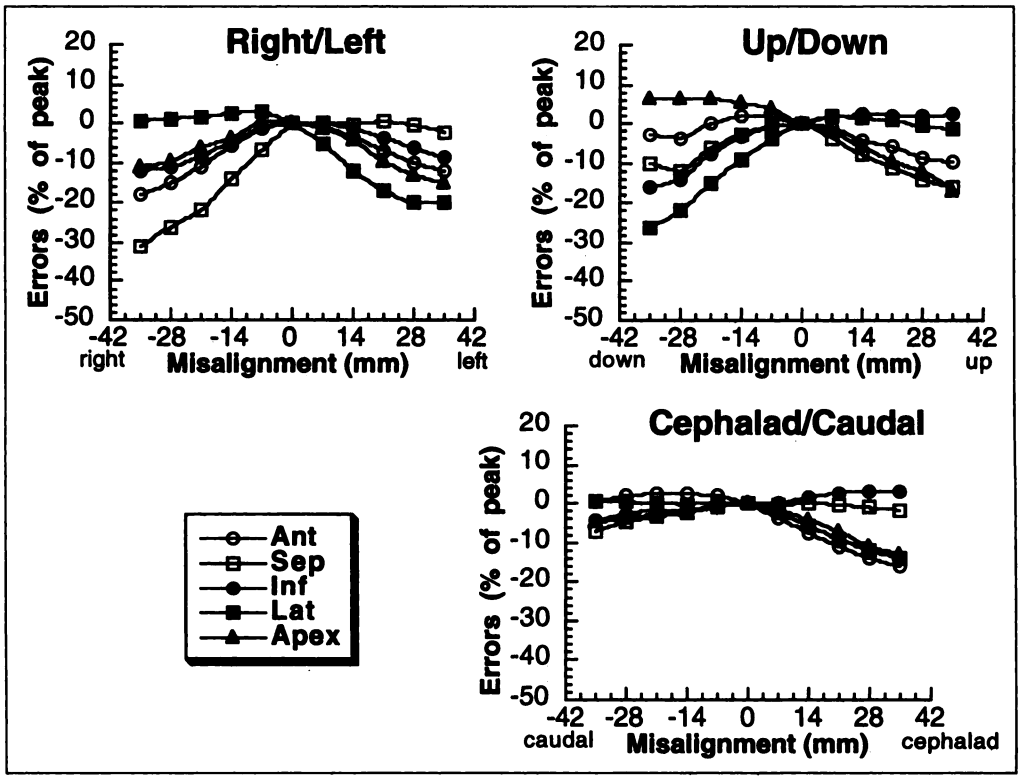

FIGURE 5. Changes in relative regional activity, as a function of misalignment between transmission and emission data, are shown for each of five segments and are an average of all 10 patients. The directions shown on each graph indicate the direction in which the emission data have been shifted relative to the transmission data.

images. It should be noted, however, that these results are based on a simple phantom without factors confounding the interpretation of data (e.g., variation in thorax geometry). Although phantom studies would give useful information as to the effect of such misalignment in a clean situation, clinical study is important to confirm the phantom data.

Clinical Data

To date, there is little data available for the effects of misalignment between transmission and emission data on AC cardiac SPECT images in humans (*13*). As expected from the phantom data, misalignment between the transmission and emission data produced errors in measured activity on AC emission images. The severity and extent of errors, however, was less significant in humans than that observed in the phantom. This is explained by blurring in both transmission and emission data caused by cardiac motion, by breathing and by different thorax structures of patients from that of the most simplified chest phantom. In one PET study (*14*), estimates for range of expected misalignments due to repositioning patients between transmission and emission scans were reportedly x, $y < 6$ mm and for $z < 11$ mm. If the misalignments are kept small (within 7-mm or 1-pixel), the errors may be kept under 10%. However, a 14-mm (2-pixel) shift readily causes up to 14% error in the measurement. It should be noted that these errors are an averaged value from all 10 patients. Therefore, the severity of errors differs from patient to patient, depending on details of body habitus, etc., and some patients show a greater magnitude of errors than what was reported as an averaged value (Tables 1–3).

In addition to these observations, a shift along the z-axis (cephalad/caudal) appears to cause less distortion per pixel of shift than does the equivalent x (right/left) and y (up/down) shifts. This is in agreement with a PET study assessing errors in the emission data caused by misalignment between the transmission and emission scans (*15*). This is probably because a displacement along the z-axis does not produce as large a

TABLE 1
Error in Relative Regional Activity Caused by Misalignment (21 mm) Between Transmission and Emision Data Along X-Axis

		Anterior		Septal		Inferior		Lateral		Apex	
Patient no.	Sex	Right	Left	Right	Left	Right	Left	Right	Left	Right	Left
1	M	−9.7	−4.0	−21.7	0.4	−6.7	−1.6	3.5	−13.5	−2.7	−9.5
2	M	−17.0	−10.0	−28.0	1.5	−12.2	−8.9	−5.8	−21.4	−8.7	−10.3
3	M	−9.2	−4.2	−23.8	3.9	−7.4	1.2	0.3	−20.5	−9.0	−11.0
4	F	−8.7	−1.6	−19.8	1.0	−3.5	−3.1	3.0	−11.3	−5.0	−6.4
5	F	−8.5	−5.6	−19.0	−1.4	−8.0	−3.0	−0.7	−18.6	−5.6	−7.3
6	M	−6.2	−10.6	−10.4	3.6	−6.2	−1.4	5.3	−14.8	−0.6	−5.8
7	M	−7.4	−9.2	−18.3	0.6	−7.8	−4.1	1.9	−16.3	−5.1	−11.9
8	M	−11.6	−9.2	−30.5	−7.4	−10.4	−10.1	6.1	−18.8	−5.5	−12.1
9	M	−12.3	−12.9	−23.0	−1.6	−11.1	−8.6	4.0	−25.2	−12.2	−20.6
10	M	−16.7	−2.6	−25.7	4.1	−11.7	3.5	−2.6	−12.3	−8.2	−2.7
Mean ± s.d.		−10.8 ± 3.7	−7.0 ± 3.9	−22.0 ± 5.7	0.5 ± 3.4	−8.5 ± 2.8	−3.6 ± 4.4	1.5 ± 3.7	−17.1 ± 4.5	−6.2 ± 3.3	− 9.8 ± 5.0

Values indicate errors in relative regional activity (% of peak activity) introduced by a 21-mm misalignment.

TABLE 2
Error in Relative Regional Activity Caused by Misalignment (21 mm) Between Transmission and Emision Data Along Y-Axis

		Anterior		Septal		Inferior		Lateral		Apex	
Patient no.	Sex	Down	Up	Down	Up	Down	Up	Down	Up	Down	Up
1	M	0.3	−3.0	−9.4	−13.0	−7.7	3.8	−12.8	4.6	6.0	−2.0
2	M	3.4	−6.8	−1.4	−10.9	−2.5	1.8	−8.9	−2.8	7.0	−12.4
3	M	0.9	−6.1	−5.0	−12.0	−3.7	0.4	−18.6	−1.1	8.2	−12.2
4	F	−4.2	−9.6	−2.5	−15.1	−15.9	−3.9	−24.4	−0.2	−4.1	−12.7
5	F	−3.2	−6.7	−7.2	−11.7	−13.7	0.7	−21.8	−1.1	5.2	−11.4
6	M	−0.3	−3.3	−3.9	−4.1	−2.7	7.1	−8.7	3.3	8.0	−5.8
7	M	−1.4	−8.1	−9.8	−11.4	−6.5	1.0	−16.3	−1.4	6.4	−12.2
8	M	2.8	−4.3	−7.3	−14.7	−11.6	3.0	−14.7	6.4	6.4	−4.3
9	M	4.1	−2.1	−5.4	−3.2	−5.5	7.3	−10.0	4.3	9.6	−9.8
10	M	−1.8	−9.3	−11.7	−10.0	−6.8	1.6	−17.0	−2.5	11.6	−11.9
Mean ± s.d.		0.1 ± 2.8	−5.9 ± 2.7	−6.4 ± 3.4	−10.6 ± 4.0	−7.7 ± 4.7	2.3 ± 3.3	−15.4 ± 5.3	1.0 ± 3.4	6.4 ± 4.2	−9.4 ± 3.9

Values indicate errors in relative regional activity (% of peak activity) introduced by a 21-mm misalignment.

movement of myocardium into the lung field as does x or y movement depending on heart axis orientation.

Study Limitations

There are several limitations in our study. First, it is uncertain to what extent the results with the uniform cardiac phantom we used are applicable to the phantom with defects. We did not investigate the effects of misalignment in patients having perfusion defects. Second, the small number of patients studied precluded us from performing a gender-specific analysis of misalignment effects in a meaningful way. Third, patient motion during acquisition was not considered in our study, which may also cause additional artifacts. Finally, our current software did not allow for the assessment of the effect of rotational misalignment. These issues need to be addressed in any further phantom and clinical studies.

Implications of the Study

Attenuation correction using measured attenuation maps is one of the most important developments in recent SPECT technology. When it is applied to cardiac SPECT imaging, an improved diagnostic accuracy can be expected by reducing attenuation artifacts. There are several approaches proposed for the attenuation correction (*1,2,9*). Some of these use sequential imaging of transmission and emission scans (*16*), and others use simultaneous transmission and emission measurement (*9*). When sequential imaging is performed, misalignment between transmission and emission scans can be caused by patient motion. As reported in this study, it is obvious that such patient motion can cause serious errors in measured activity in AC SPECT. In this regard, simultaneous transmission and emission measurement, rather than separate acquisition, is preferable because it virtually eliminates errors caused by patient motion between the scans.

With multidetector SPECT systems, transmission and emission images are simultaneously acquired using separate heads as is the case in our system and others (*1,2*). Misalignment between the camera heads is minimized by routine quality control, including center-of-rotation correction. When using nonparallel-hole collimators, such as fanbeam or offset fanbeam collimators, precision measurements must be performed to determine the exact localization and stability of the transmission source relative to the focus of the fanbeam collimator. If this is not assured, misalignment between transmission and emission projections will result after rebinning to parallel hole geometry, and this will introduce errors in measured activity on the reconstructed AC SPECT images. Depending on varying geometrical errors, different distortions of the reconstructed transmission data can be observed as shown in Figure 6. It is also noteworthy that this effect is not constant for each location in the transmission image. In addition, pixel size and homogeneity of fanbeam and parallel-hole collimators must be determined to avoid mismatching of reconstructed attenuation maps and emission images. Routine quality assurance, including fanbeam parameters, is important in systems with simultaneous

TABLE 3
Error in Relative Regional Activity Caused by Misalignment (21 mm) Between Transmission and Emision Data Along Z-Axis

		Anterior		Septal		Inferior		Lateral		Apex	
Patient no.	Sex	Caudal	Cephalad	Caudal	Cephalad	Caudal	Cephalad	Caudal	Cephalad	Caudal	Cephalad
1	M	6.6	−10.3	−2.5	1.7	1.5	6.1	2.6	−4.0	0.5	−5.1
2	M	3.5	−11.6	−0.8	0.5	−0.7	3.6	−1.5	−11.1	−1.7	−13.8
3	M	2.6	−8.8	−4.4	−0.4	−5.9	6.5	−0.7	−10.6	−1.3	−11.5
4	F	5.0	−14.1	−3.4	−4.6	−1.6	2.2	−1.5	−13.6	−3.2	−10.2
5	F	0.2	−12.7	−4.7	−3.4	−0.1	0.8	−0.4	−11.4	−3.4	−6.5
6	M	0.3	−15.5	−2.6	3.5	−4.0	0.0	0.2	−12.0	−3.9	−2.7
7	M	3.5	−13.3	−5.2	−1.3	−5.6	−0.2	0.1	−9.9	−5.3	−4.6
8	M	1.4	−8.0	−1.8	−3.9	1.6	−2.0	2.4	−7.2	−1.2	−13.9
9	M	2.4	−9.4	−1.2	0.3	1.7	0.8	0.2	−5.7	−3.5	−5.5
10	M	−0.2	−9.6	−6.7	4.6	−4.0	8.9	−0.7	−6.2	−3.7	0.3
Mean ± s.d.		2.5 ± 2.2	−11.3 ± 2.4	−3.3 ± 1.9	−0.3 ± 3.1	−1.7 ± 3.0	2.7 ± 3.5	0.1 ± 1.4	−9.2 ± 3.2	−2.7 ± 1.7	−7.3 ± 4.8

Values indicate errors in relative regional activity (% of peak activity) introduced by a 21-mm misalignment.

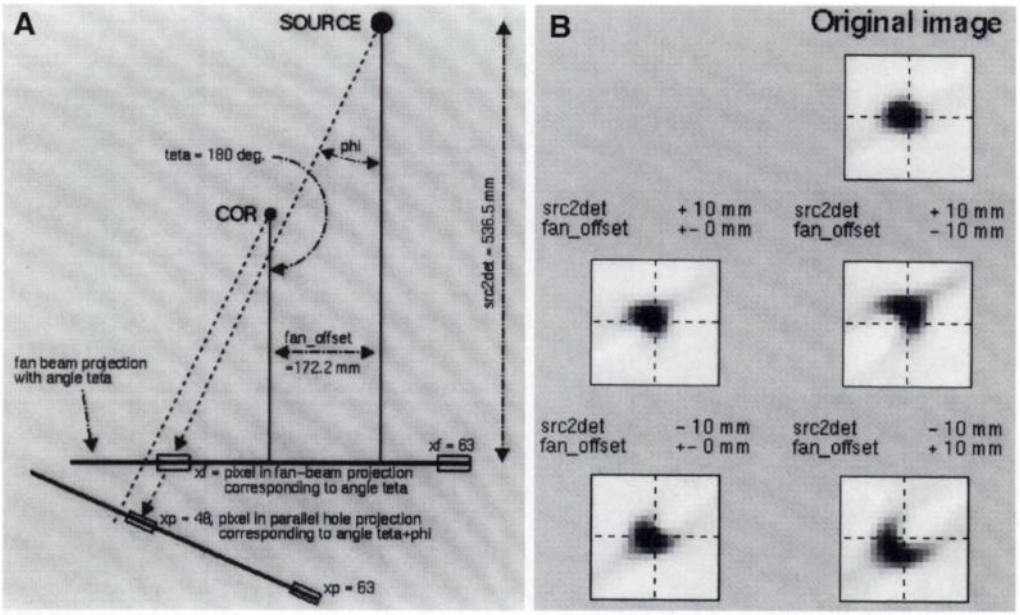

FIGURE 6. (A) Schematic of the fanbeam geometry for the transmission measurement. Errors in the rebinned parallel hole projection data can be introduced by either those in source/detector distance (src2det) or in fan_offset. COR indicates the center of rotation. (B) Effects of wrong geometrical values on the reconstructed transmission image of a lead rod. The upper right image displays the reconstructed transmission image without errors. The images displayed in the middle and lower rows represent misaligned transmission data due to the wrong values for the distance between the transmission source and detector (src2det) and/or for the fan_offset. The wrong geometrical parameters introduce not only translocation but also distortion of the transmission data.

transmission and emission measurement capability in order to avoid such artifacts.

CONCLUSION

The results of our study indicate that it is essential for the accurate diagnosis of AC cardiac SPECT images to ensure that there is no geometrical error between transmission and emission data.

ACKNOWLEDGMENTS

We thank Dr. Claire S. Duvernoy for her comments during manuscript preparation. Dr. Matsunari was supported by Mitsubishi Research Institute, Japan.

REFERENCES

1. Bacharach S, Buvat I. Attenuation correction in cardiac positron emission tomography and single-photon emission computed tomography. *J Nucl Cardiol* 1995;2:246–255.
2. King M, Tsui B, Pan T. Attenuation compensation for cardiac single-photon emission computed tomographic imaging: part 1. Impact of attenuation and methods of estimating attenuation maps. *J Nucl Cardiol* 1995;2:513–524.
3. King M, Tsui B, Pan T, Glick S, Soares E. Attenuation compensation for cardiac single-photon emission computed tomographic imaging: part 2. Attenuation compensation algorithms. *J Nucl Cardiol* 1996;3:55–63.
4. Ficaro EP, Fessler JA, Shreve PD, Kritzman JN, Rose PA, Corbett JR. Simultaneous transmission/emission myocardial perfusion tomography. Diagnostic accuracy of attenuation-corrected 99mTc-sestamibi single-photon emission computed tomography. *Circulation* 1996;93:463–473.
5. Matsunari I, Stollfuss J, Schneider-Eicke J, et al. Resting technetium-99m tetrofosmin myocardial SPECT with and without attenuation correction for detecting viable myocardium: comparison with FDG-PET [Abstract]. *J Am Coll Cardiol* 1996;27:163A.
6. Diamond G, Forrester J. Analysis of probability as an aid in the clinical diagnosis of coronary artery disease. *N Engl J Med* 1979;300:283–298.
7. Boning G, Ficaro E, Nekolla S, et al. Attenuation correction for a multihead SPECT system: initial validation [abstract]. *J Nucl Med* 1995;36:11P.
8. Ficaro E, Hawman E, Schwaiger M. Simultaneous transmission/emission tomography using a line source with an off-center fanbeam collimator [Abstract]. *J Nucl Med* 1994;35:191P.
9. Ficaro EP, Fessler JA, Ackermann RJ, Rogers WL, Corbett JR, Schwaiger M. Simultaneous transmission-emission thallium-201 cardiac SPECT: effect of attenuation correction on myocardial tracer distribution. *J Nucl Med* 1995;36:921–931.
10. Fessler J. Penalized weighted least-squares image reconstruction for positron emission tomography. *IEEE Trans Signal Proc* 1993;13:290–300.
11. Laubenbacher C, Rothley J, Sitomer J, et al. An automated analysis program for the evaluation of cardiac PET studies: initial results in the detection and localization of coronary artery disease using nitrogen-13-ammonia. *J Nucl Med* 1993;34:968–978.
12. Murase K, Tanada S, Inoue T, Sugawara Y, Hamamoto K. Effects of misalignment between transmission and emission scans on SPECT images. *J Nucl Med Technol* 1993;21:152–156.
13. Kemerink G, Bacharach S, Carson R. Effects of attenuation scan misalignment in cardiac SPECT [Abstract]. *J Nucl Med* 1990;31:875P.
14. Buvat I, Freedman NM, Dilsizian V, Bacharach SL. Realignment of emission contaminated attenuation maps with uncontaminated attenuation maps for attenuation correction in PET. *J Comp Assist Tomog* 1996;20:848–854.
15. McCord ME, Bacharach SL, Bonow RO, Dilsizian V, Cuocolo A, Freedman N. Misalignment between PET transmission and emission scans: its effect on myocardial imaging. *J Nucl Med* 1992;33:1209–1214.
16. Prvulovich EM, Lonn AHR, Bomanji JB, Jarrit PH, Ell PJ. Effect of attenuation correction on myocardial thallium-201 distribution in patients with a low likelihood of coronary artery disease. *Eur J Nucl Med* 1997;24:266–275.